Supplementary Information

Zinc-1,4-Benzenedicarboxylate-Bipyridine Frameworks – Linker Functionalization Impacts Network Topology During Solvothermal Synthesis

Sebastian Henke,[a] Andreas Schneemann,[a] Shobhna Kapoor,[b] Roland Winter[b] and Roland A. Fischer*[a]

[a] *Lehrstuhl für Anorganische Chemie II – Organometallics and Materials Chemistry, Ruhr-Universität Bochum, 44780 Bochum, Germany.*
[b] *Lehrstuhl für Physikalische Chemie I, Technische Universität Dortmund, 44227 Dortmund, Germany.*

Contents

1 Single Crystal Data of $[Zn_2(2,3\text{-BME-bdc})_2(bipy)]_n$

Table S1: Crystal data of $[Zn_2(2,3\text{-BME-bdc})_2(bipy)]_n$ (**2as**) determined by single crystal X-ray diffraction (CCDC 834509).

Empirical formula	C19 H20 N O8 Zn
Formula weight	455.73
Temperature	108 K
Wavelength	0.71073 Å
Crystal system	tetragonal
Space group	*P*4/mmm
Unit cell dimensions	*a* = 10.773(4) Å; α = 90°
	b = 10.773(4) Å; β = 90°
	c = 13.947(5) Å; γ = 90°
Volume	1619(10) $Å^3$
Z	2
Density (calculated)	0.936 g/cm^3
Absorption coefficient	0.788 mm^{-1}
F(000)	470
Crystal dimensions	0.12 x 0.05 x 0.01 mm^3
Theta range for data collection	3.48° to 24.99°
Reflections collected	6647
Independent reflections	885
Reflections observed (>2σ)	519
Data completeness	98.8%
Absorption correction	multi-scan
Refinement method	full-matrix least-squares on F^2
Data / parameters / restrains	885 / 73 / 48
Goodness-of-fit on F^2	0.658
R-indices [I>2σ(I)]	R^1 = 0.0348; wR2 = 0.0520
R-indices (all data)	R^1 = 0.0873; wR2 = 0.0663

Most of the atoms in the crystal structure of **2as** are disordered. The carboxylate groups are disordered over two positions. Furthermore, the aromatic rings of 2,3-BME-bdc and bipy are disordered over four positions. Due to this severe disorder the flexible 2-methoxyethoxy chains could not be located in the structure refinement. However, the flexible substituents have been included in the molecular formula and molecular weight. To account for the electron density, assignable to the disordered side chains, as well as the DMF and EtOH guest molecules, the diffraction data have been treated with the SQUEEZE routine in Platon.[1]

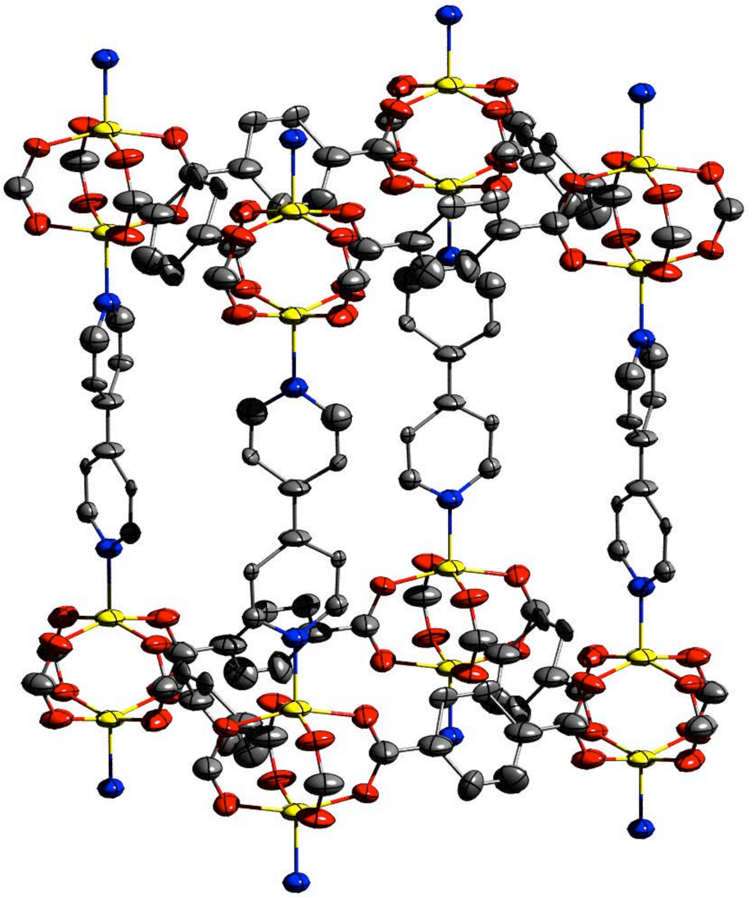

Figure S1: Ellipsoid plot of the structure of **2as**. Zinc, oxygen, nitrogen and carbon atoms are shown in yellow, red, blue and grey, respectively. The ellipsoids are shown at the 50% probability level. The carboxylate groups are disordered over two positions and the aromatic moieties of 2,3-BME-bdc and bipy disordered over four positions. However, only one set of the disordered moieties is shown. The flexible 2-methoxyethoxy chains are highly disordered and could not be localized in the structure refinement.

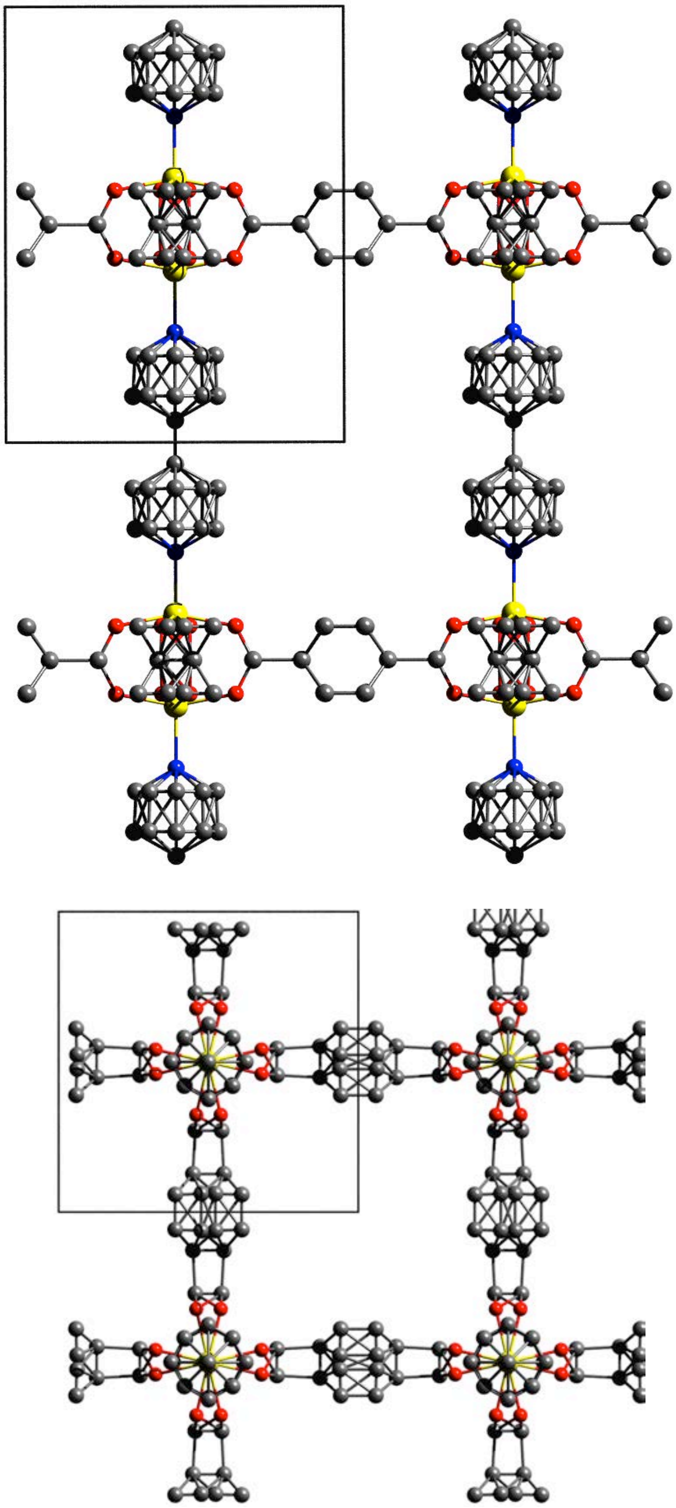

Figure S2: Packing diagrams of a 2x2x2 super cell of **2as**. View in [100] direction (top) and [001] direction (bottom). The carboxylate groups of the linker are disordered over two positions. Furthermore, the aromatic rings of bipy and 2,3-BME-bdc are disordered over four positions. Hence, the flexible 2-methoxyethoxy groups could not be located in the structure refinement due to severe disorder. Carbon, nitrogen, oxygen and zinc atoms are shown in dark grey, blue, red, and yellow, respectively.

2 Single Crystal Data of $[Zn_2(DM\text{-}bdc)_2(bipy)]_n$

Table S2: Crystal data of $[Zn_2(DM\text{-}bdc)_2(bipy)]_n$ (**4as**) determined by single crystal X-ray diffraction (CCDC 834510).

Empirical formula	C15 H12 N O6 Zn
Formula weight	367.65
Temperature	107 K
Wavelength	0.71073 Å
Crystal system	monoclinic
Space group	*C*2/m
Unit cell dimensions	*a* = 11.78(2) Å; α = 90°
	b = 18.24(3) Å; β = 123.97(10)°
	c = 8.280(7) Å; γ = 90°
Volume	1475(4) $Å^3$
Z	4
Density (calculated)	1.655 g/cm^3
Absorption coefficient	1.696 mm^{-1}
F(000)	748
Crystal dimensions	0.10 x 0.06 x 0.03 mm^3
Theta range for data collection	2.97° to 27.49°
Reflections collected	5907
Independent reflections	1724
Reflections observed (>2σ)	953
Data completeness	99.0%
Absorption correction	multi-scan
Refinement method	full-matrix least-squares on F^2
Data / parameters / restrains	1724 / 163 / 48
Goodness-of-fit on F^2	1.018
R-indices [I>2σ(I)]	R^1 = 0.0906; wR2 = 0.1535
R-indices (all data)	R^1 = 0.1803; wR2 = 0.1903

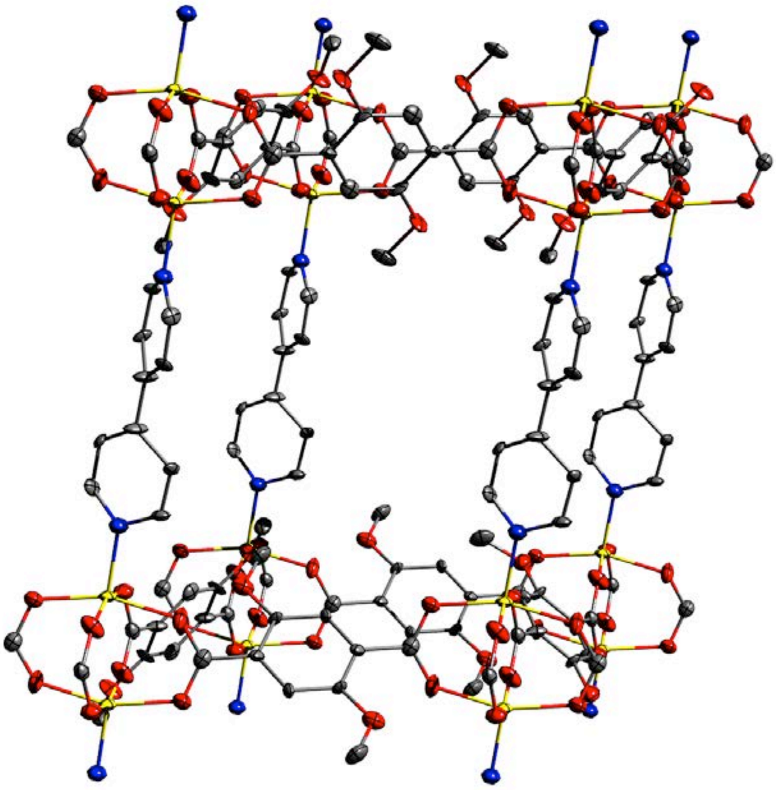

Figure S3: Ellipsoid plot of the structure of **4as**. Zinc, oxygen, nitrogen and carbon atoms are shown in yellow, red, blue and grey, respectively. The ellipsoids are shown at the 50% probability level. The aromatic moieties of DM-bdc and bipy, as well as the methoxy groups are disordered over two positions. However, only one set of the disordered moieties is shown. Hydrogen atoms, as well as the second interpenetrating framework have been omitted for clarity.

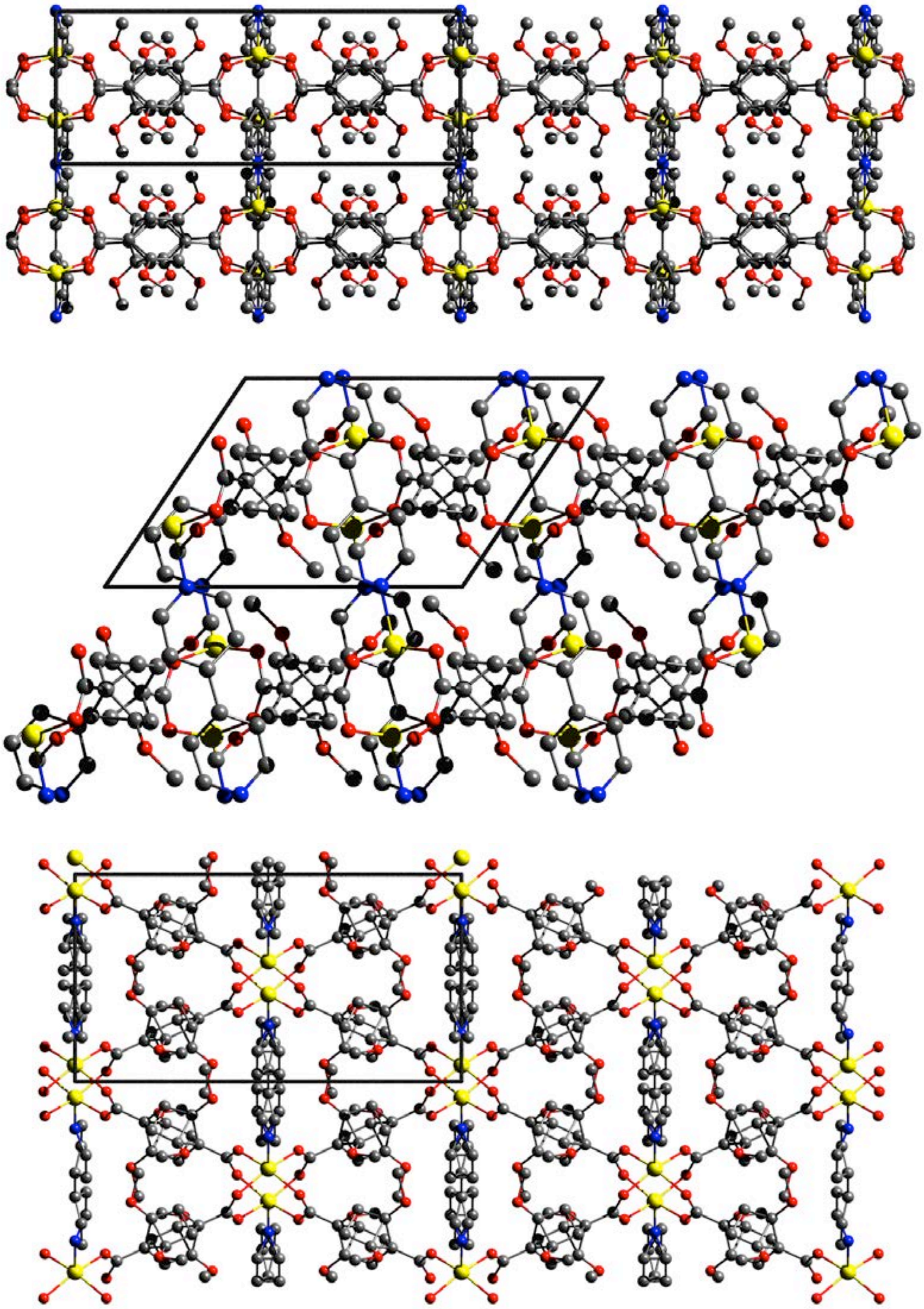

Figure S4: Packing diagrams of a 2x2x2 super cell of **4as**. View in [100] direction (top), [010] direction (middle), and [001] direction (bottom). The aromatic rings of bipy and DM-bdc, as well as the methoxy substituents of DM-bdc are disordered over two positions. Carbon, nitrogen, oxygen and zinc atoms are shown in dark grey, blue, red, and yellow, respectively. Hydrogen atoms are omitted for the sake of clarity.

3 Powder Diffraction Data

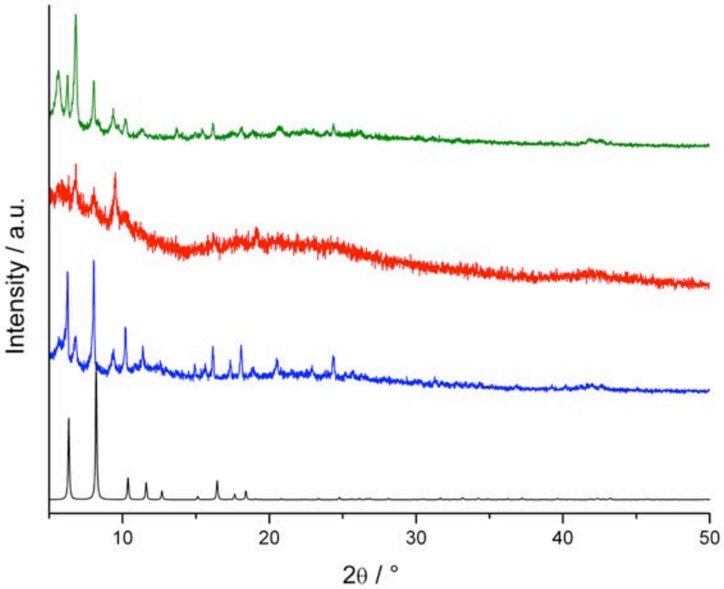

Figure S5: PXRD patterns of **2as** (blue), **2dry** (red), and a DMF reinfiltrated sample DMF@**2dry** (green) in comparison to the pattern calculated from the single crystal structure of **2as** (black). Interestingly, compound **2** looses its crystallinity upon drying. This can be attributed to the large void volume of **2as** according to the single crystal structure and the increased flexibility of the donor-functionalized framework.[2] We suggest, that the crystalline structure of **2as** is only stable when guest molecules are present. However, reinfiltration of DMF in **2dry** over gas phase does recover crystallinity of the sample, but the material seems to transfer (partially) to a different structure as visualized by the diffraction pattern of DMF@**2dry**. Nevertheless, a detailed analysis of the structural transitions, which occur upon drying and resolvation of **2** turned out to be very complex and is beyond the scope of this work.

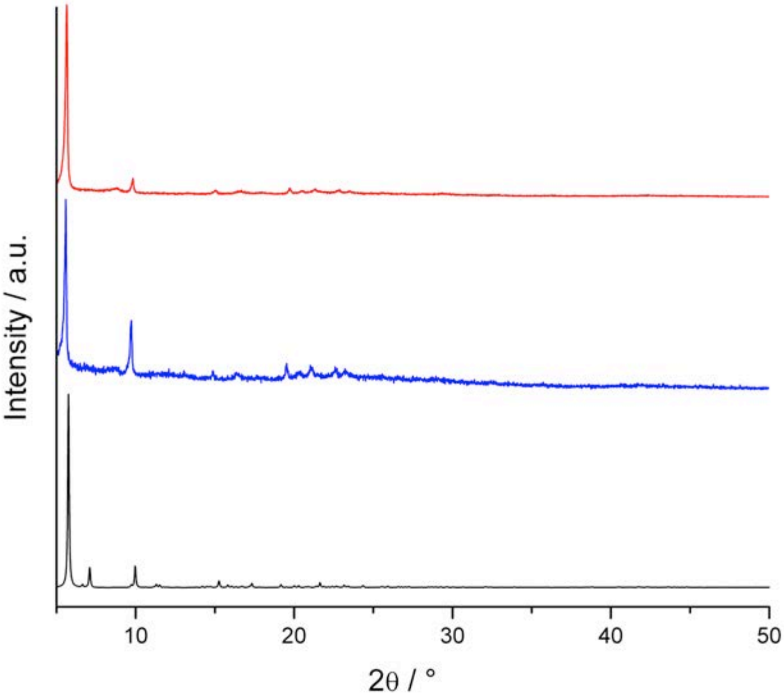

Figure S6: PXRD patterns of **3as** (blue) and **3dry** (red) in comparison to the pattern calculated from the single crystal structure of **1as** (black).

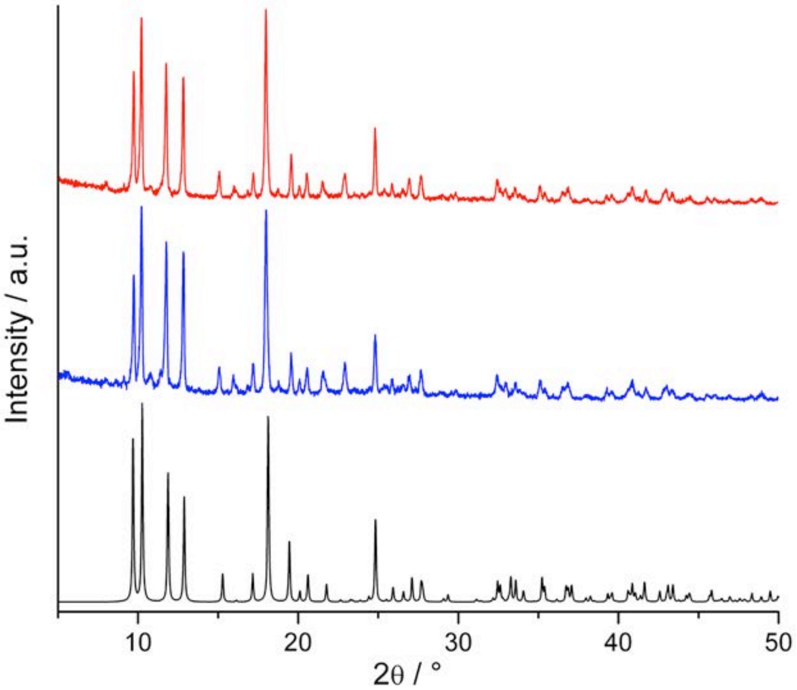

Figure S7: PXRD patterns of **4as** (blue) and **4dry** (red) in comparison to the pattern calculated from the single crystal structure of **4as** (black).

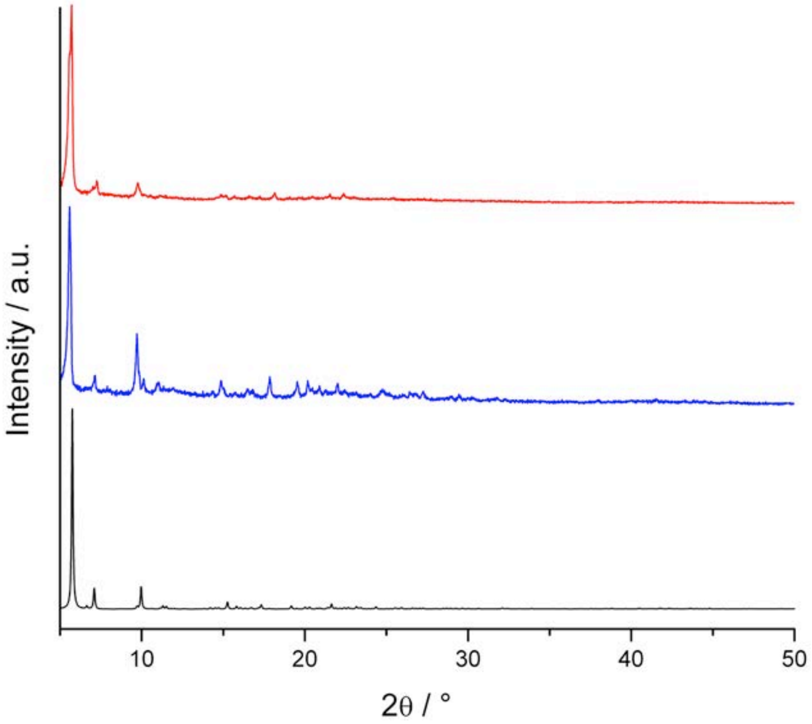

Figure S8: PXRD patterns of **5as** (blue) and **5dry** (red) in comparison to the pattern calculated from the single crystal structure of **1as** (black).

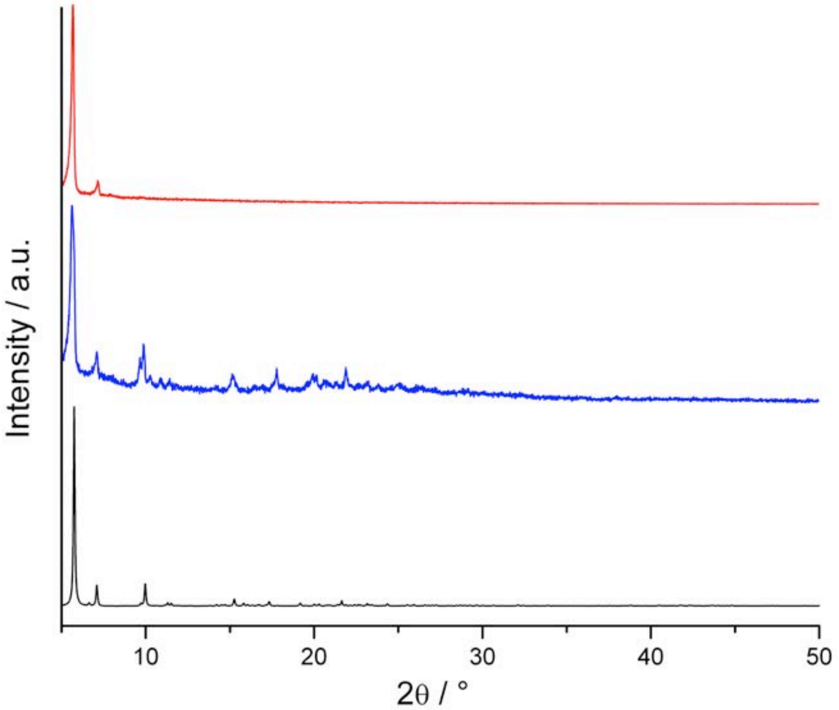

Figure S9: PXRD patterns of **6as** (blue) and **6dry** (red) in comparison to the pattern calculated from the single crystal structure of **1as** (black).

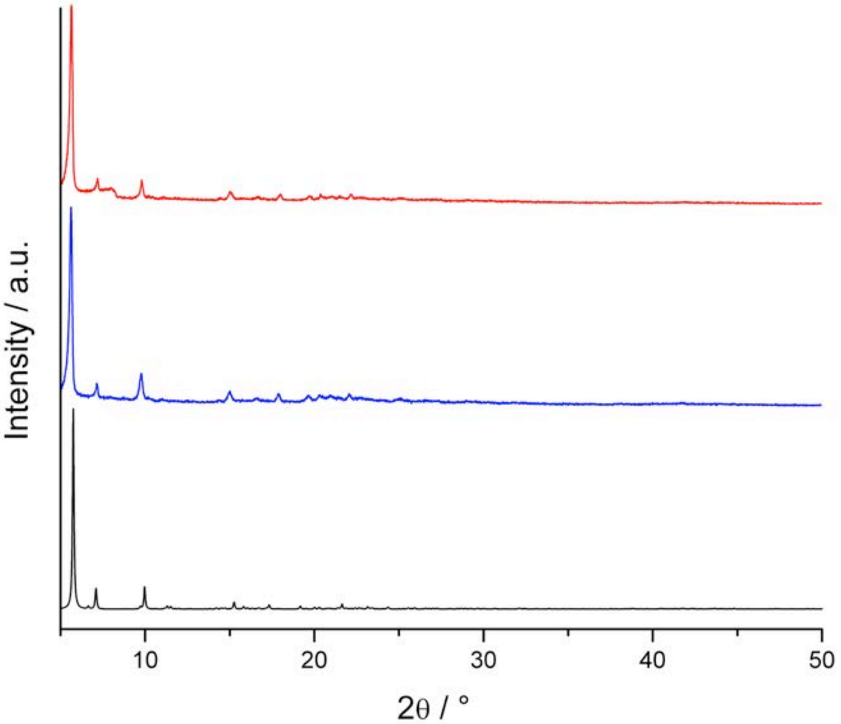

Figure S10: PXRD patterns of **7as** (blue) and **7dry** (red) in comparison to the pattern calculated from the single crystal structure of **1as** (black).

Table S3: Results of indexation of the PXRD patterns of **3as**, **5as**, **6as**, and **7as** followed by cell parameter refinement with Celref.[3]

Compound	**3as**	**5as**	**6as**	**7as**
Space group	*R*-3c	*R*-3c	*R*-3c	*R*-3c
a / Å	53.06(7)	53.75(13)	53.70(9)	53.80(11)
b / Å	53.06(7)	53.75(13)	53.70(9)	53.80(11)
c / Å	17.83(1)	17.82(1)	17.78(1)	17.76(1)
α / °	90	90	90	90
β / °	90	90	90	90
γ / °	120	120	120	120
V / Å^3	43469(67)	44590(93)	44415(89)	44515(99)

4 Thermo Gravimetric Analyses

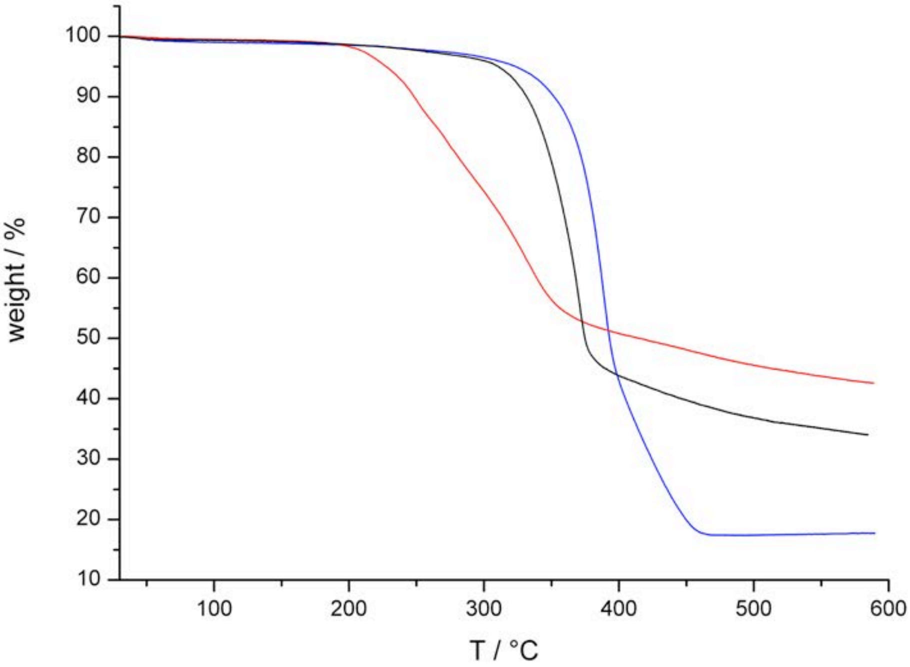

Figure S11: TGAs of the activated compounds **1dry** (black, taken from ref. 4), **2dry** (red), and **3dry** (blue).

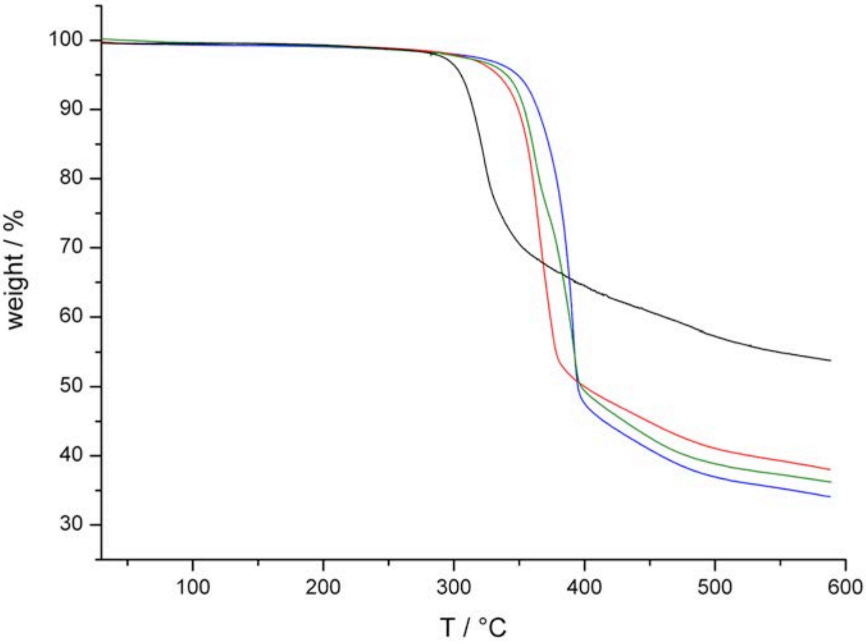

Figure S12: TGAs of the activated compounds **4dry** (black), **5dry** (red), **6dry** (blue), and **7dry** (green).

5 NMR Spectra

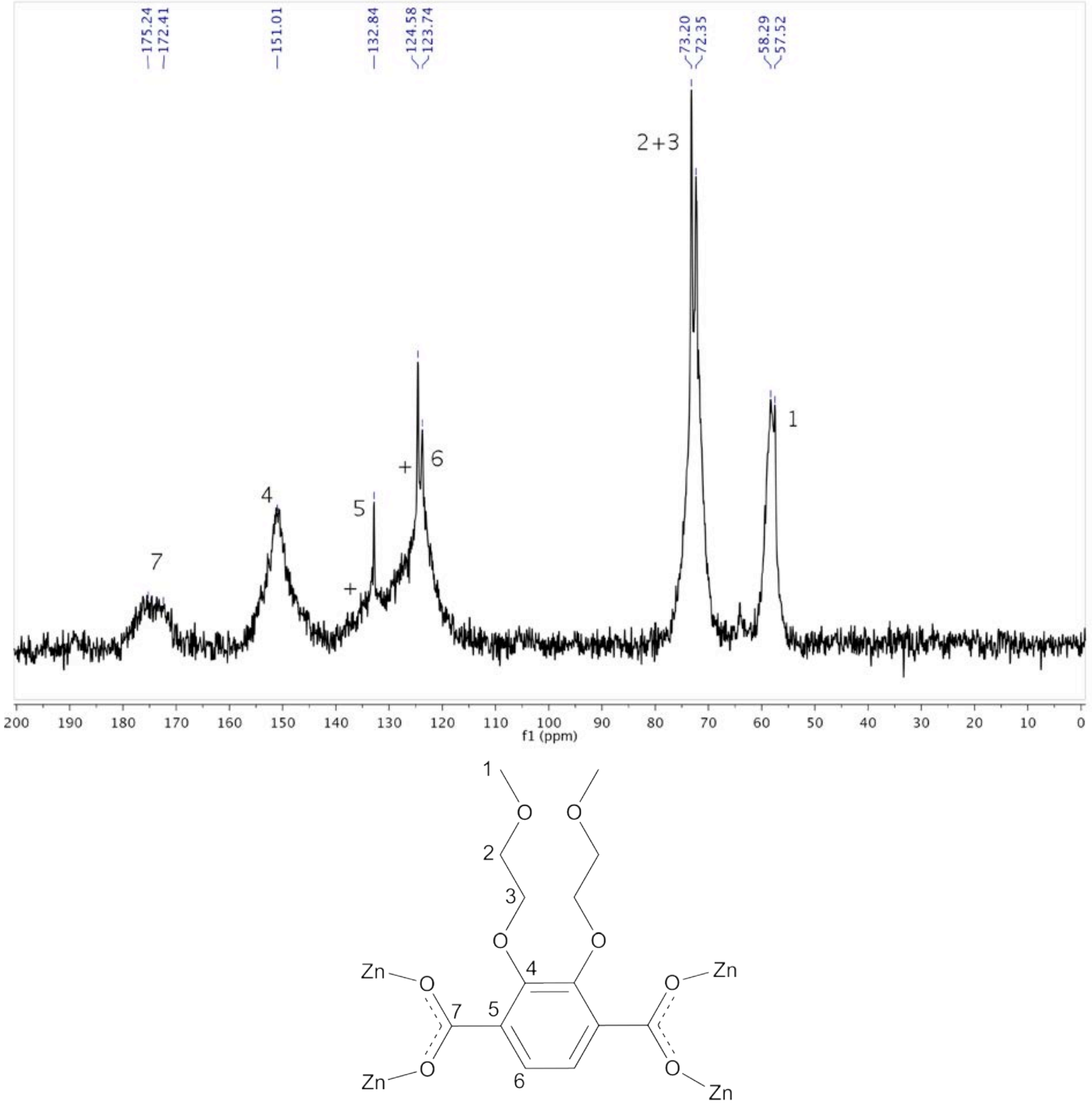

Figure S13: ^{13}C MAS NMR spectrum of **2dry**. Signals belonging to the bipy linker are marked with a cross (+). The broad signals and the bad S/N ratio are in accordance with the almost amorphous nature of the dried material.

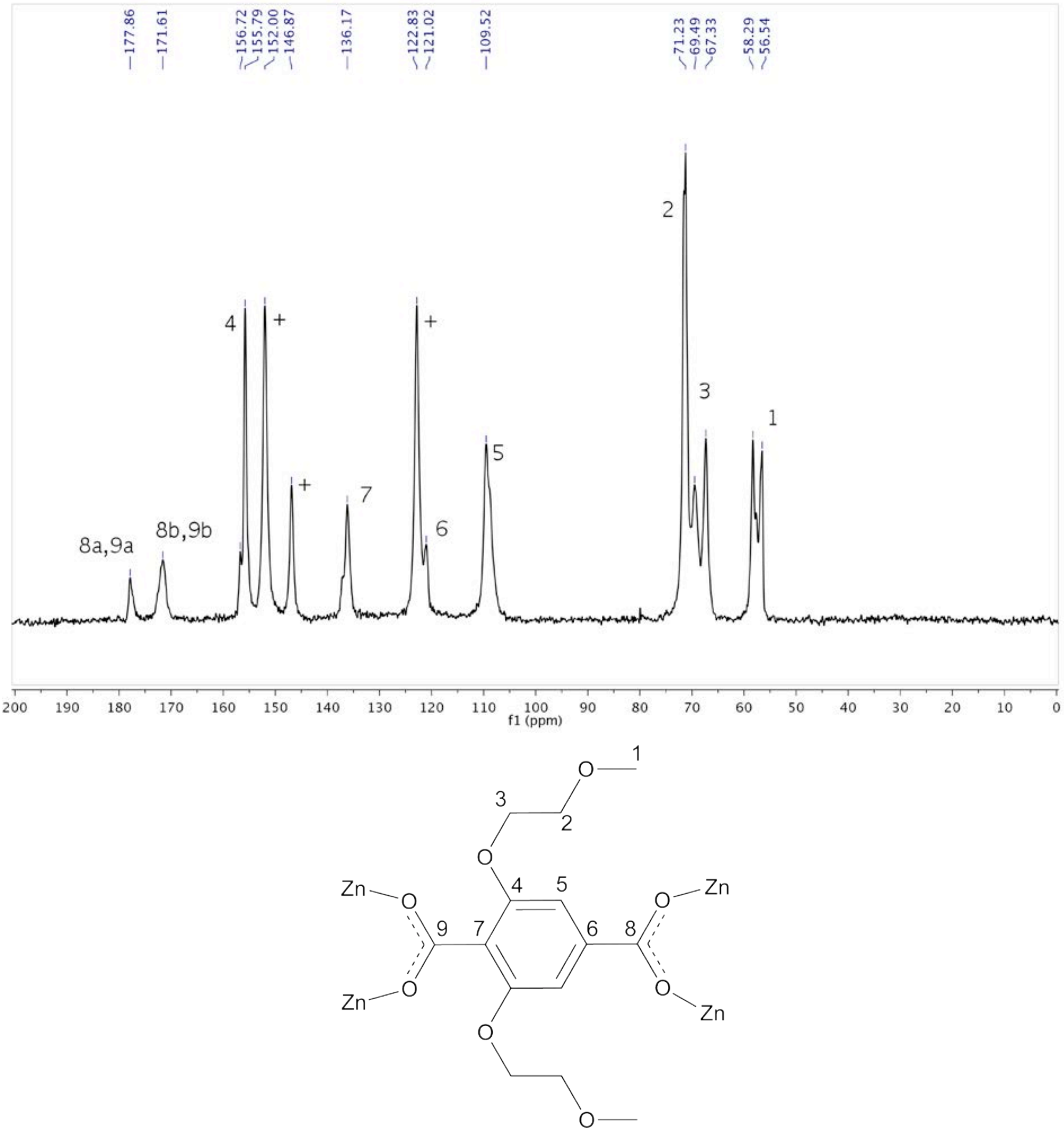

Figure S14: ^{13}C MAS NMR spectrum of **3dry**. Signals belonging to the bipy linker are marked with a cross (+). Both signals of the carboxylate carbon atoms C8 and C9 are split into two signals (C8a, C8b, C9a and C9b), because the carboxylate groups have two different coordination modes in the honeycomb-like structure. One signal corresponds to the carboxylates, which bind in a bidentate chelating fashion to one Zn atom, and the other signal to the carboxylates, which bridge two Zn centres in *syn-anti* fashion.

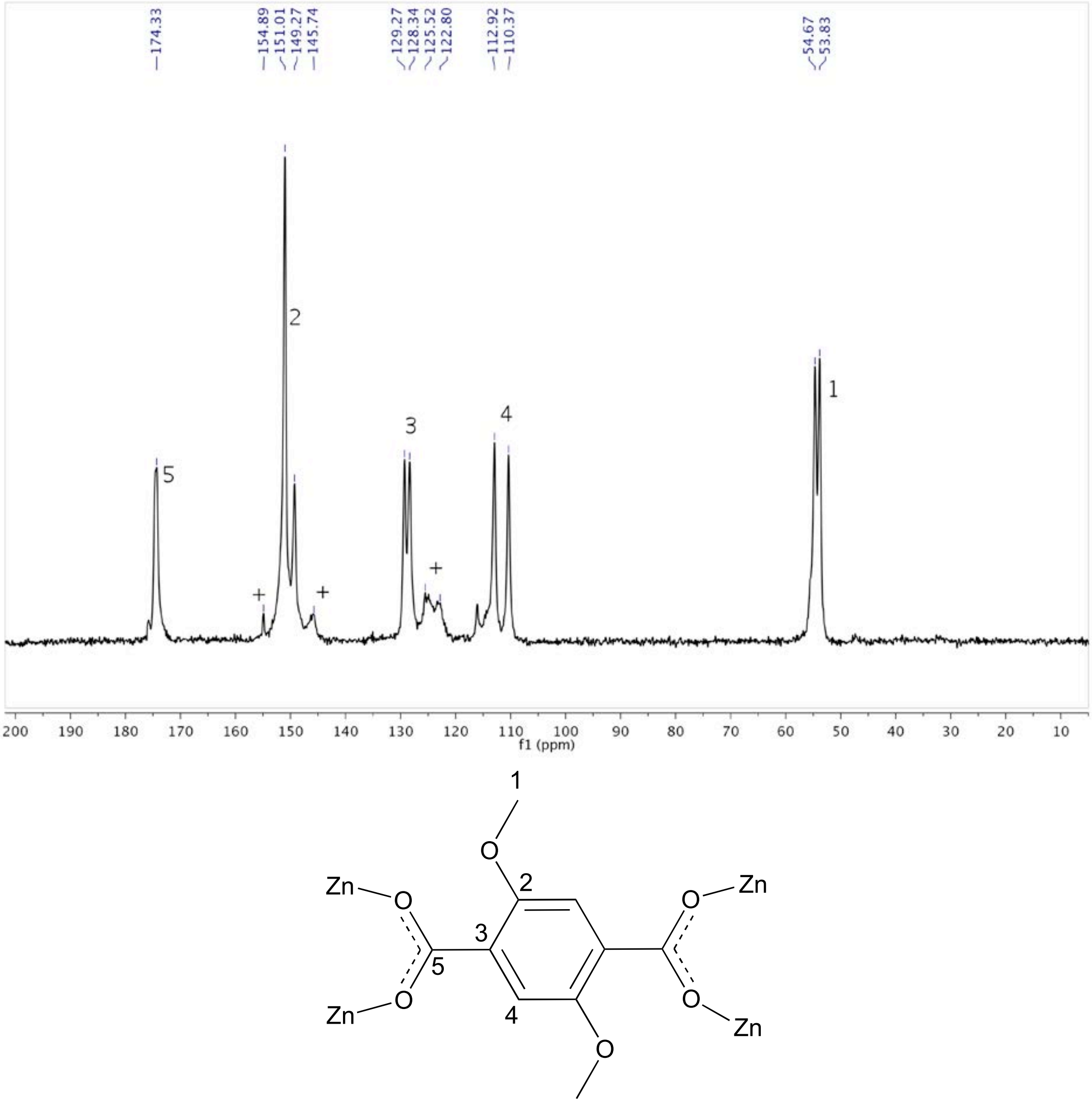

Figure S15: ^{13}C MAS NMR spectrum of **4dry**. Signals belonging to the bipy linker are marked with a cross (+).

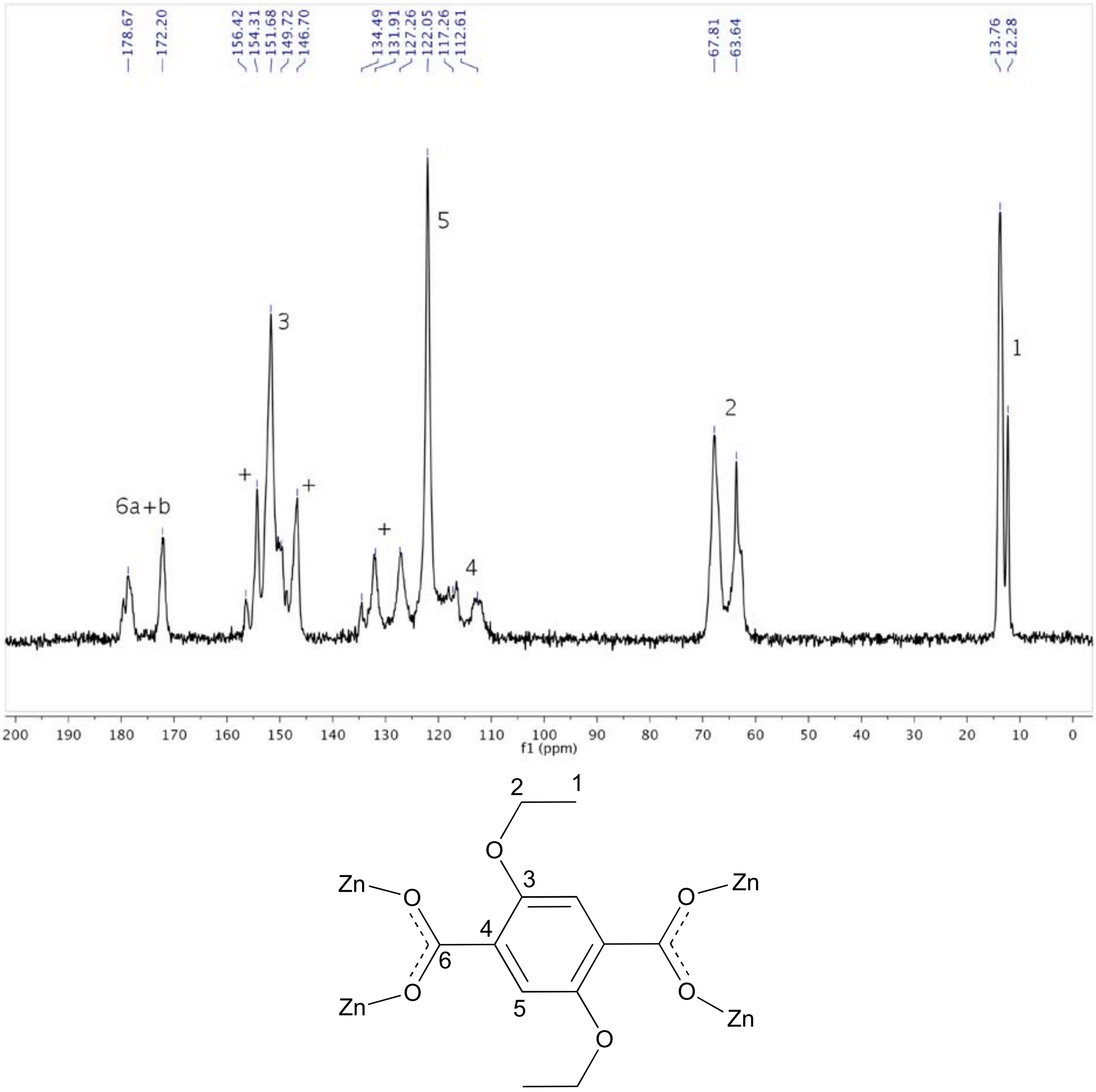

Figure S16: ^{13}C MAS NMR spectrum of **5dry**. Signals belonging to the bipy linker are marked with a cross (+).The signal of C6 is split into two individual signals (C6a and C6b), because the carboxylate groups have two different coordination modes in the honeycomb-like structure. One signal corresponds to the carboxylates, which bind in a bidentate chelating fashion to one Zn atom, and the other signal to the carboxylates, which bridge two Zn centres in *syn-anti* fashion.

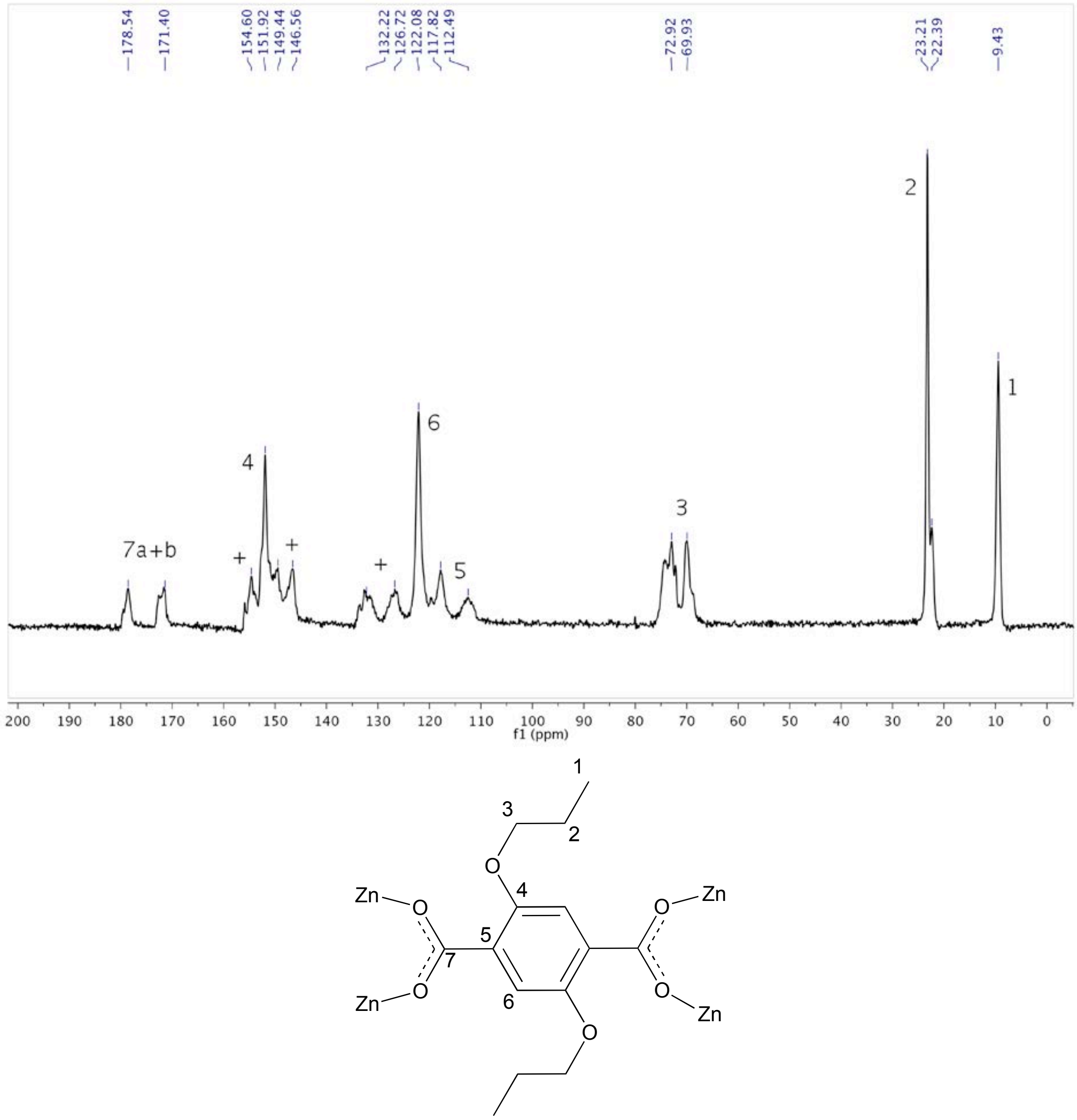

Figure S17: ^{13}C MAS NMR spectrum of **6dry**. Signals belonging to the bipy linker are marked with a cross (+).The signal of C7 is split into two individual signals (C7a and C7b), because the carboxylate groups have two different coordination modes in the honeycomb-like structure. One signal corresponds to the carboxylates, which bind in a bidentate chelating fashion to one Zn atom, and the other signal to the carboxylates, which bridge two Zn centres in *syn-anti* fashion.

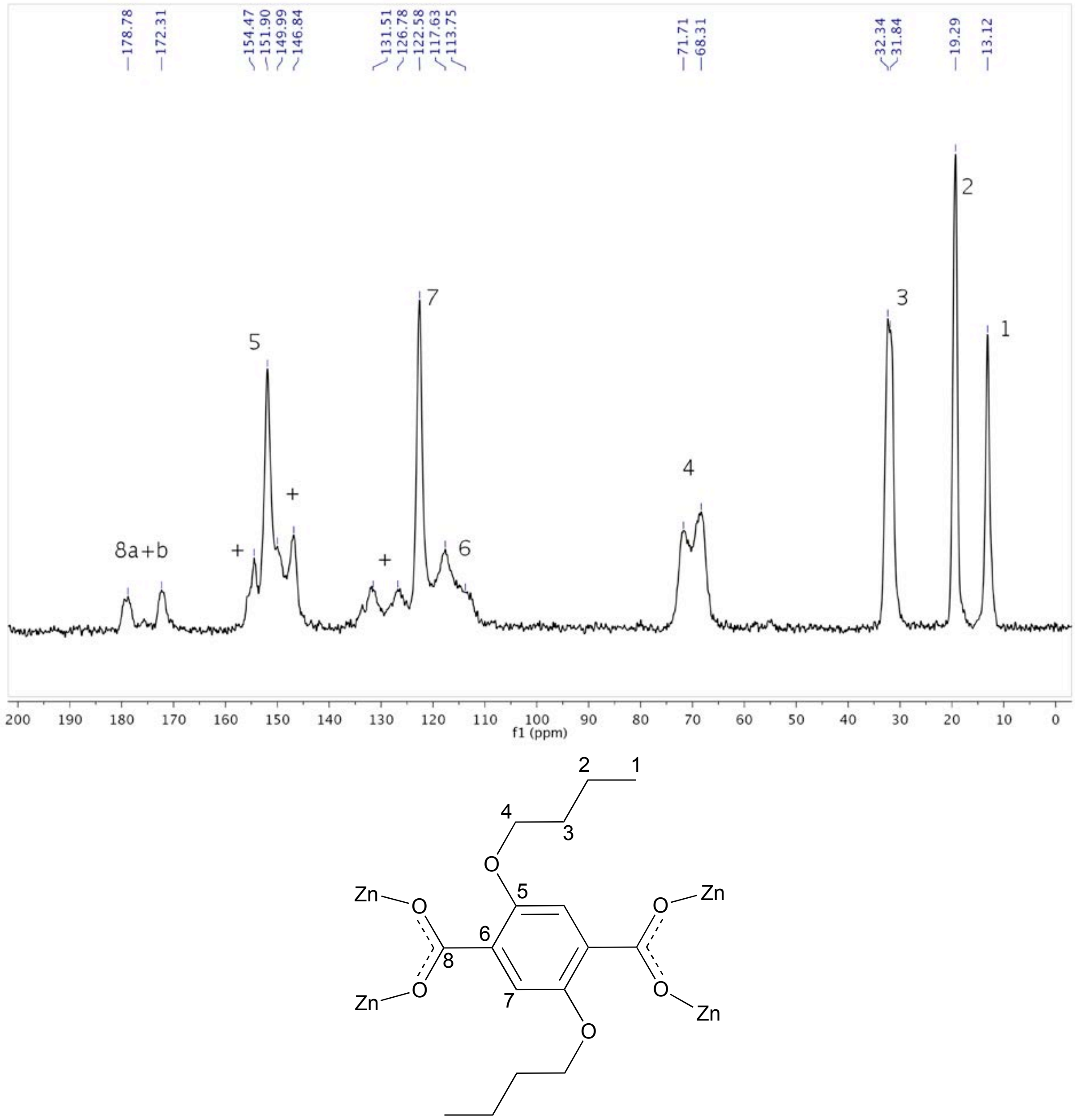

Figure S18: ^{13}C MAS NMR spectrum of **7dry**. Signals belonging to the bipy linker are marked with a cross (+).The signal of C8 is split into two individual signals (C8a and C8b), because the carboxylate groups have two different coordination modes in the honeycomb-like structure. One signal corresponds to the carboxylates, which bind in a bidentate chelating fashion to one Zn atom, and the other signal to the carboxylates, which bridge two Zn centres in *syn-anti* fashion.

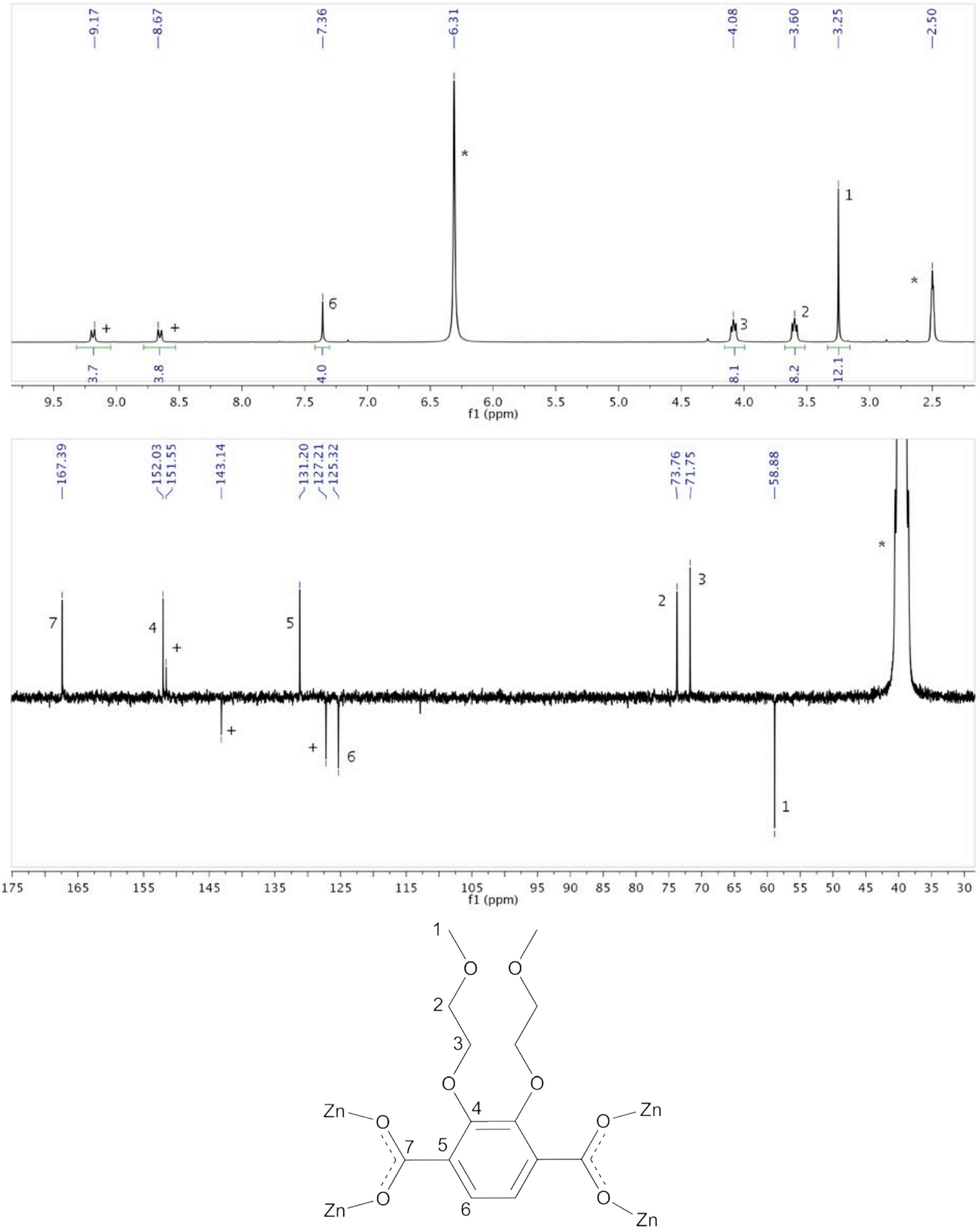

Figure S19: ^{1}H NMR (top) and ^{13}C APT NMR spectra (bottom) of a digested sample of **2dry** in 0.1 mL DCl(20%)/D_2O and 0.5 mL [D_6]DMSO. Signals belonging to the bipy linker are marked with a cross (+). Solvent signals are marked with an asterisk (*).

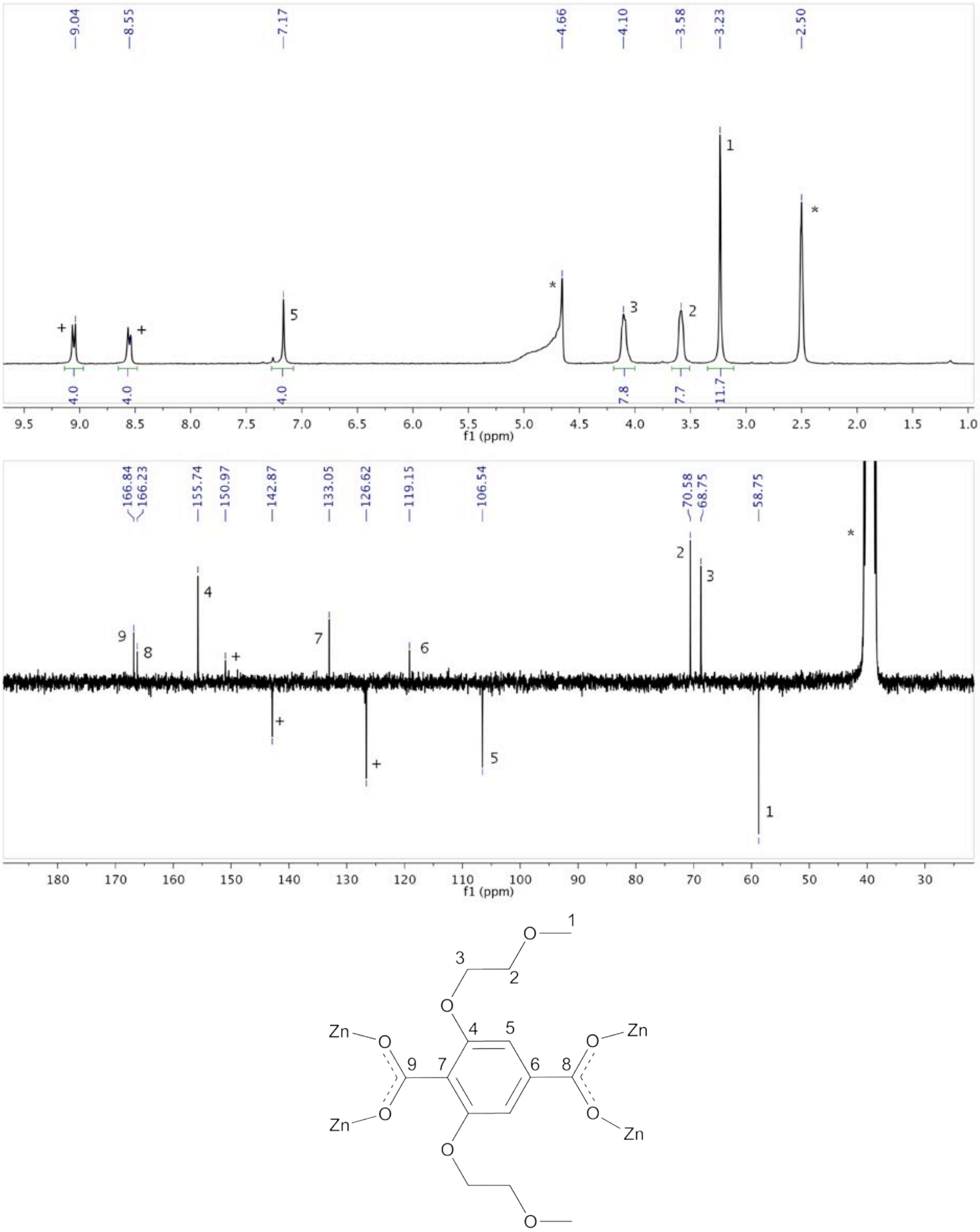

Figure S20: ^{1}H NMR (top) and ^{13}C APT NMR spectra (bottom) of a digested sample of **3dry** in 0.05 mL DCl(20%)/D_2O and 0.6 mL [D_6]DMSO. Signals belonging to the bipy linker are marked with a cross (+). Solvent signals are marked with an asterisk (*). The broad signal at approx. 4.8 ppm can be dedicated to D_2O.

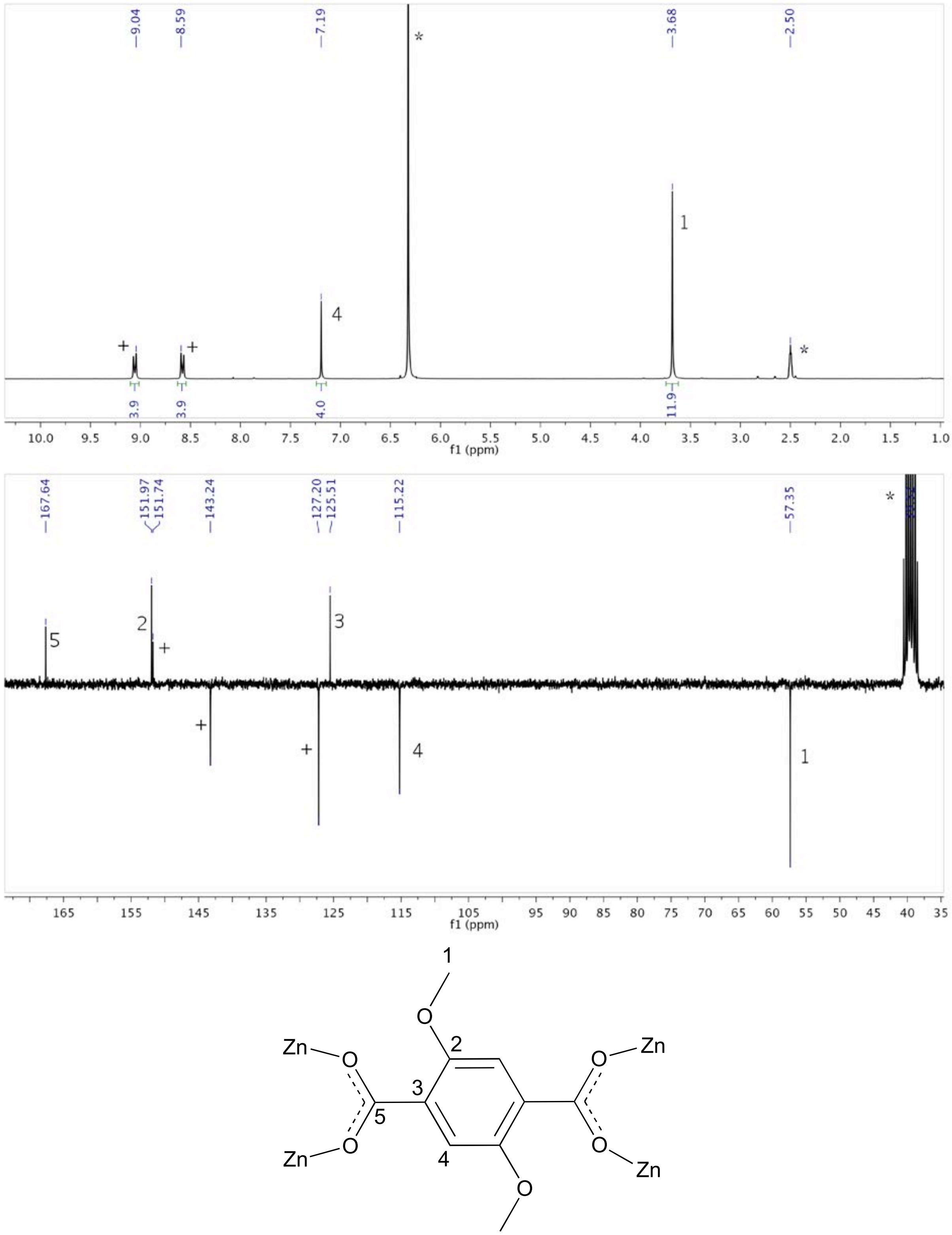

Figure S21: ^{1}H NMR (top) and ^{13}C APT NMR spectra (bottom) of a digested sample of **4dry** in 0.1 mL DCl(20%)/D_2O and 0.5 mL [D_6]DMSO. Signals belonging to the bipy linker are marked with a cross (+). Solvent signals are marked with an asterisk (*).

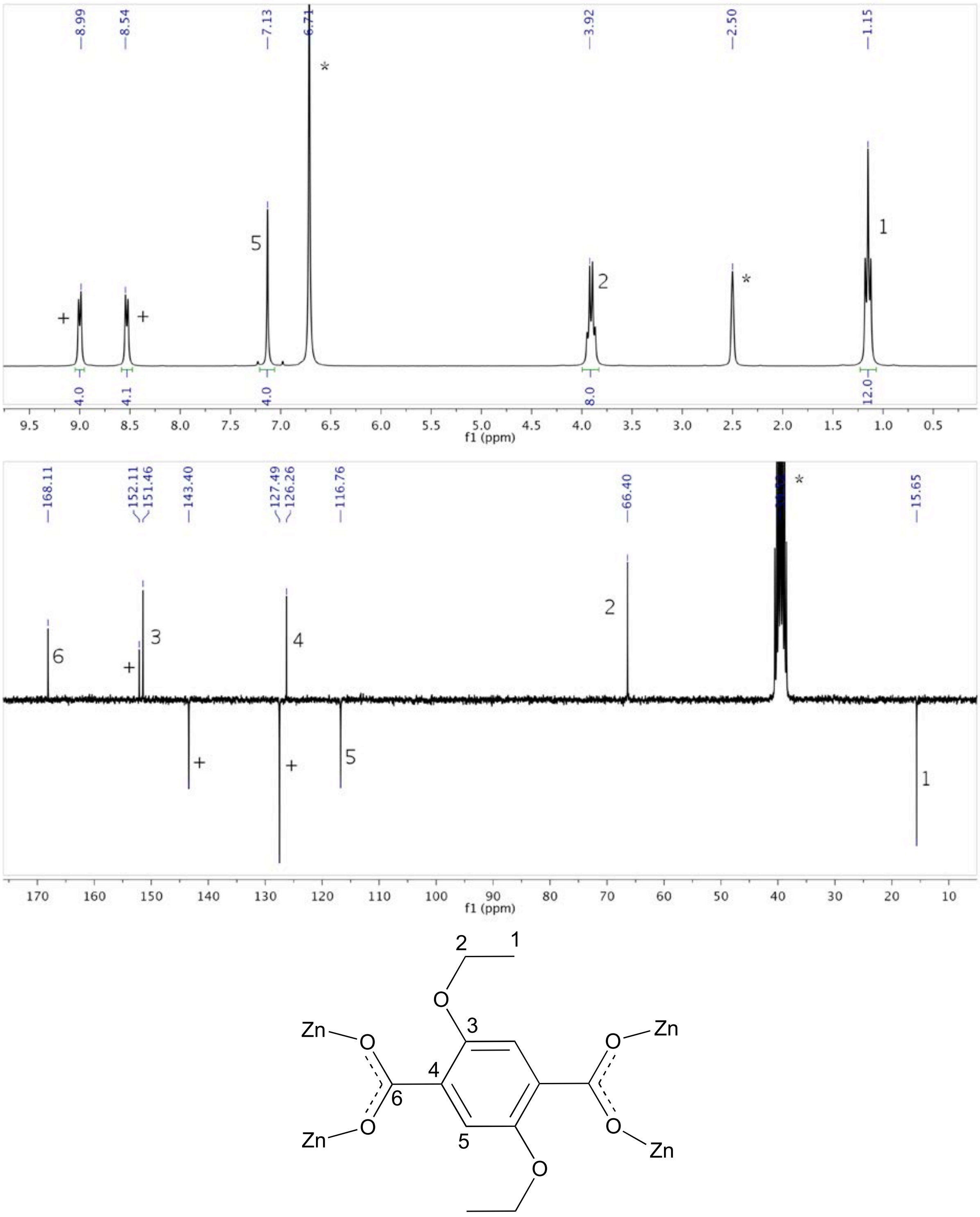

Figure S22: ^{1}H NMR (top) and ^{13}C APT NMR (bottom) spectra of a digested sample of **5dry** in 0.1 mL DCl(20%)/D_2O and 0.5 mL [D_6]DMSO. Signals belonging to the bipy linker are marked with a cross (+). Solvent signals are marked with an asterisk (*).

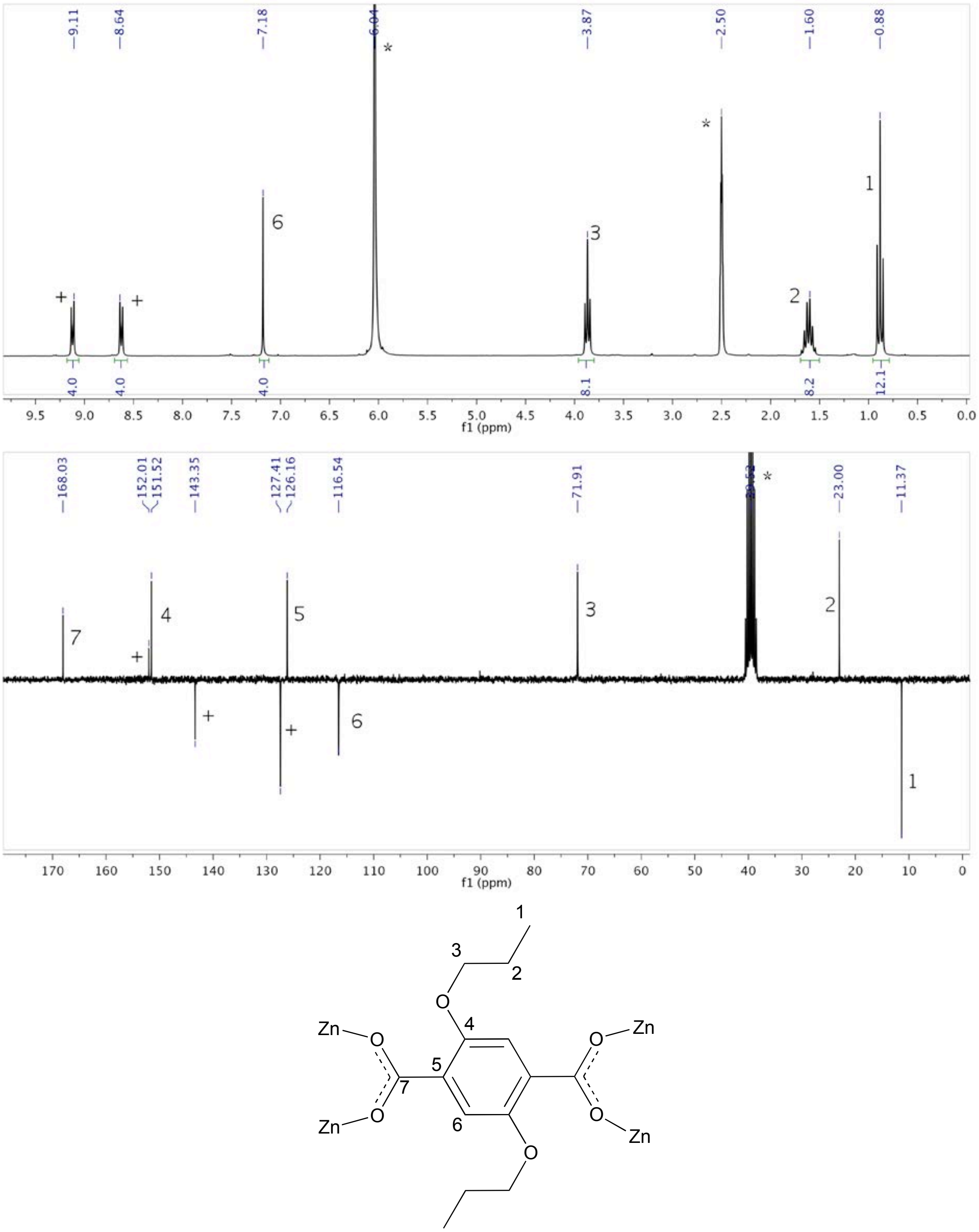

Figure S23: ^{1}H NMR (top) and ^{13}C APT NMR (bottom) spectra of a digested sample of **6dry** in 0.1 mL DCl(20%)/D_2O and 0.5 mL [D_6]DMSO. Signals belonging to the bipy linker are marked with a cross (+). Solvent signals are marked with an asterisk (*).

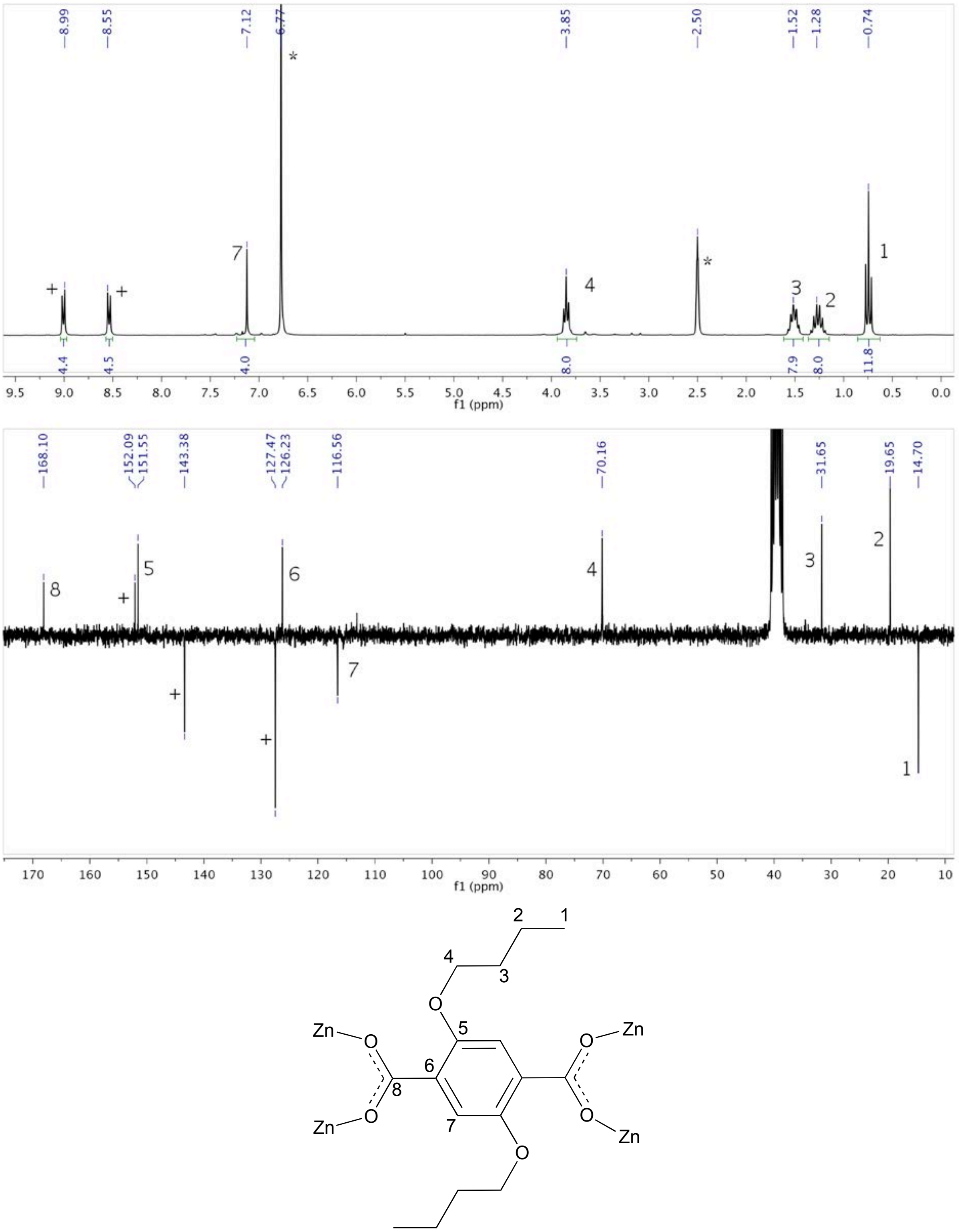

Figure S24: ^{1}H NMR (top) and ^{13}C APT NMR (bottom) spectra of a digested sample of **7dry** in 0.1 mL DCl(20%)/D_2O and 0.5 mL [D_6]DMSO. Signals belonging to the bipy linker are marked with a cross (+). Solvent signals are marked with an asterisk (*).

6 FT-IR Spectra

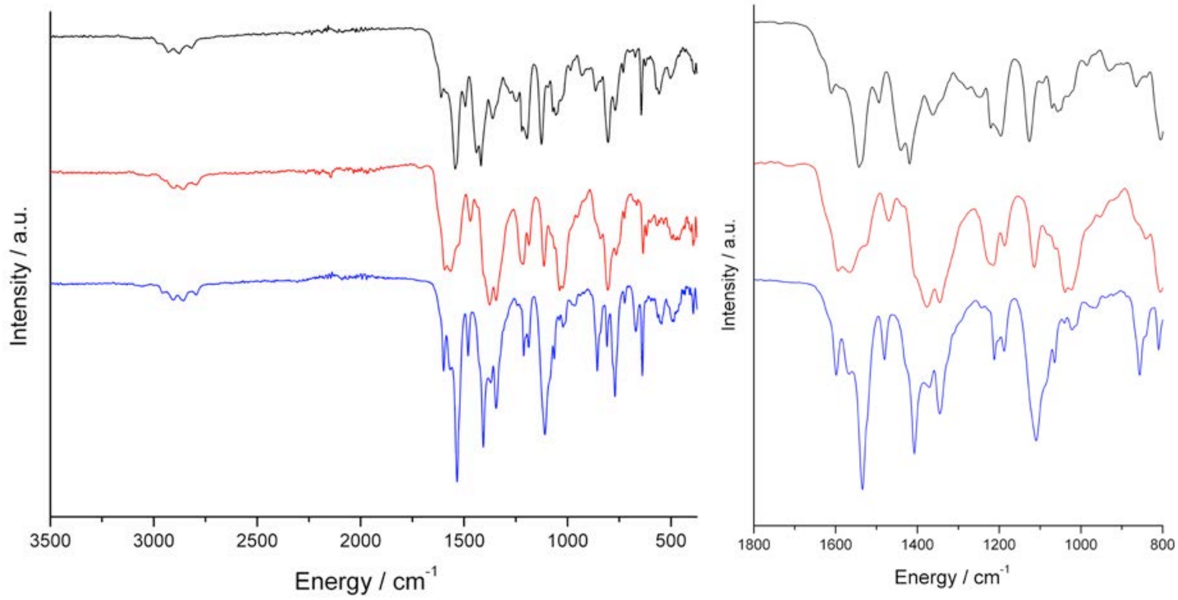

Figure S25: ATR FT-IR spectra of the activated compounds **1dry** (black, taken from ref. 4), **2dry** (red), and **3dry** (blue). The right section of the picture shows a close-up view of the vibration bands between 800 cm^{-1} and 1800 cm^{-1}.

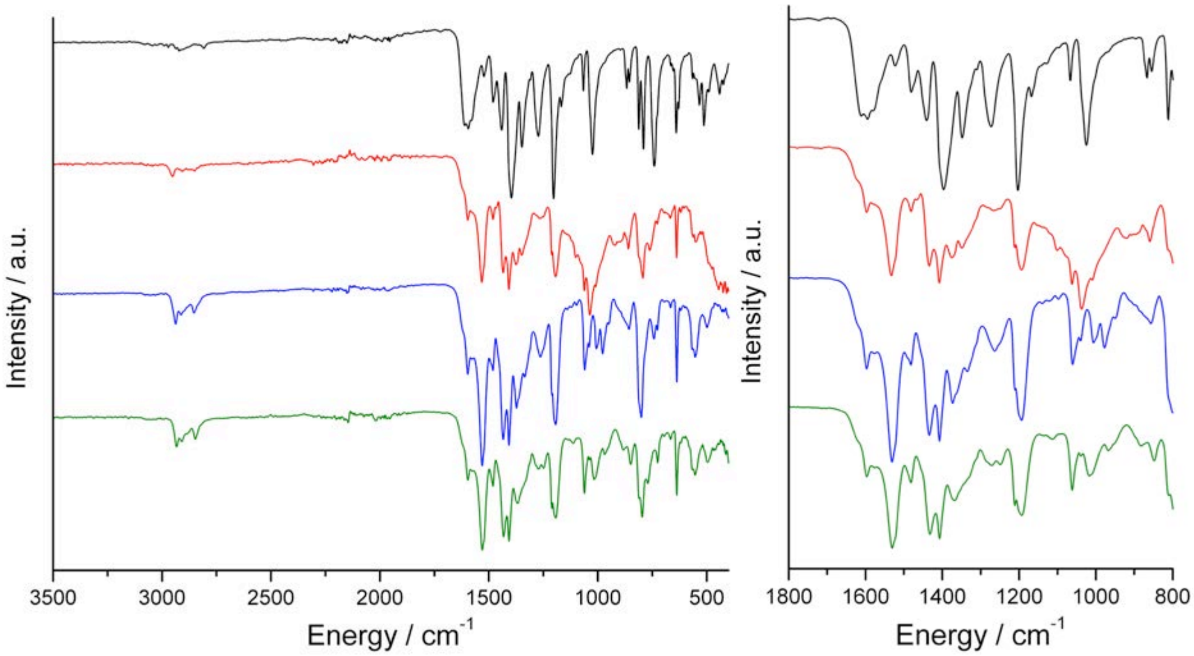

Figure S26: ATR FT-IR spectra of the activated compounds **4dry** (black), **5dry** (red), **6dry** (blue), and **7dry** (green). The right section of the picture shows a close-up view of the vibration bands between 800 cm^{-1} and 1800 cm^{-1}.

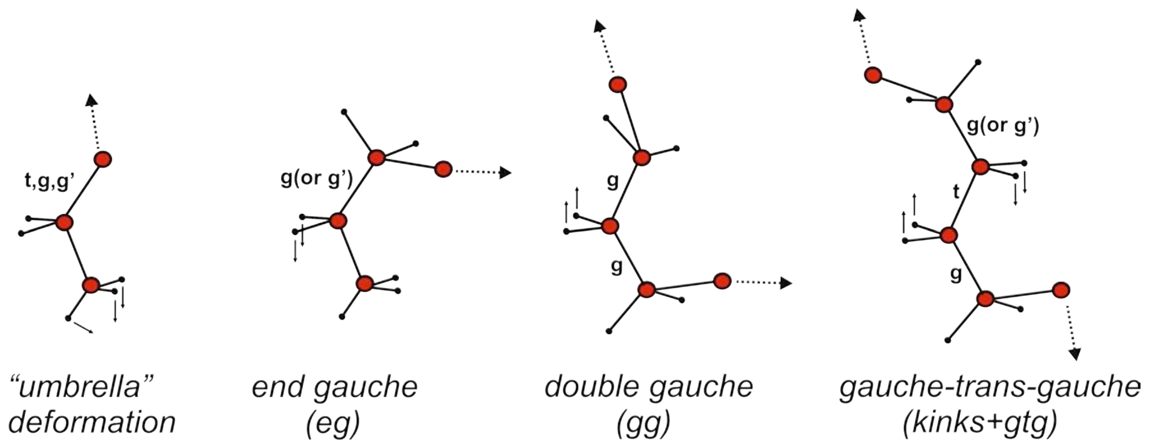

"umbrella" deformation *end gauche (eg)* *double gauche (gg)* *gauche-trans-gauche (kinks+gtg)*

Figure S27: Schematic representation of the main CH$_2$ wagging modes in the alkyl chains observed in the region 1400-1300 cm^{-1}. Solid arrows show the motion of the vibrational bands and dashed arrows indicate the possible direction of chain length propagation. (carbon; red: hydrogen; black)

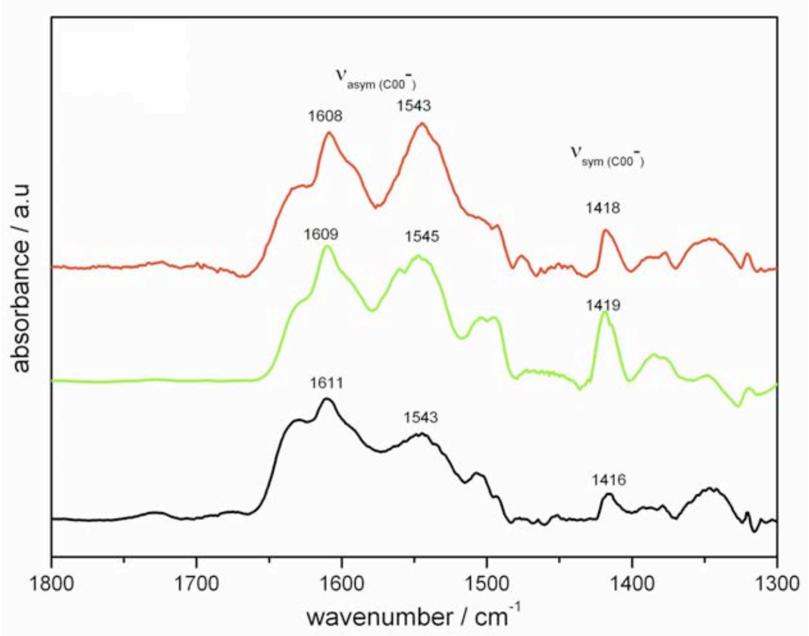

Figure S28: FT-IR spectra for the MOFs **5dry** (red), **6dry** (green), and **7dry** (black) at 25°C and ambient pressure for the wavenumber region between 1300 cm^{-1} and 1800 cm^{-1} showing characteristic bands for the $\nu_{asym(COO^-)}$ and $\nu_{sym(COO^-)}$ stretching vibrations.

Table S4: Carboxylate asymmetric and symmetric vibrational bands (wavenumbers in cm^{-1}).

MOF	$\nu_{asym(COO^-)}$	$\nu_{sym(COO^-)}$	$\Delta\nu_{MOF}$
7dry	1611, 1543	1416	195, 127
6dry	1609, 1545	1419	190, 126
5dry	1608, 1543	1418	191, 125

References

[1] A. L. Spek, *Acta Cryst.* **2009**, D65, 148-155.

[2] S. Henke, R. Schmid, J.-D. Grunwaldt, R. A. Fischer, *Chem. Eur. J.* **2010**, 16, 14296-14306.

[3] J. Laugier and B. Bochu, *LMGP-Suite, Suite of Programs for the interpretation of X-ray Experiments*, ENSP/Laboratoire des Matériaux et du Génie Physique, France, BP 46. 38042 Saint Martin d'Hères, http://www.inpg.fr/LMGP and http://www.ccp14.ac.uk/tutorial/lmgp/.

[4] S. Henke, R. A. Fischer, *J. Am. Chem. Soc.* **2011**, *133*, 2064-2067.